ORIGINAL RESEARCH PAPER

# The effect of Mn doping on structural, magnetic and optical properties of $TiO_2$ nanoparticles

***Alireza Razeghizadeh, Elham Elahi, Vahdat Rafee ****

*Department Physics, Faculty of science, Payamenoor University, IRAN*

Received: 2017-10-31 Accepted: 2018-02-08 Published: 2018-06-30

**ABSTRACT**

The aim of this paper is to study the effect of Mn concentration on the structural, magnetic and optical properties of $TiO_2$ nanoparticles. $TiO_2$ nanopowders with Mn concentration of 0%, 0.2%, 1% and 5% were synthesized by the sol-gel method. The structural, surface morphology and average crystal grain size, optical, magnetic properties and chemical compounds of the samples are studied using XRD, FE-SEM, Uv-Vis, VSM and EDX analysis respectively. The results indicate that the samples are crystallized at anatase phase. Also, the average size of the nanoparticles is decreased by increasing Mn doping percent. The study of the optical properties shows that the absorption maximum dislocates toward higher wavelengths by adding Mn to the sample. This shift may be ascribed to the enhanced trapped electron absorption caused by the Mn-doped ions. The optical energy band gap of the doping samples shows significant reduction rather the pure state. The samples show significant paramagnetic behavior when the Mn concentration is 5%.

**Keywords:** *Mn-doped, $TiO_2$ Nano-powders, Sol-gel method, Magnetic properties.*



**How to cite this article**

*Razeghizadeh A, Elahi E, Rafee V. The Effect of Mn Doping on Structural, Magnetic and Optical Properties of $TiO_2$ Nanoparticles. J. Nanoanalysis., 2018; 5(2): 77-83.* DOI: 10.22034/jna.2018.541852

## INTRODUCTION

$TiO_2$ is a safe substance for human and environment. This material has industrial importance because of having the energy band gap 3.2 e V (at anatase phase), considerable chemical resistance, and the high number of the solvents in a wide range of PH, transmittance and the high refraction coefficient [1-3]. $TiO_2$ exists in three crystallite forms: anatase, rutile, and brookite [4]. Anatase type $TiO_2$ is a crystalline structure as the tetragonal system and is photochemically more active than the others. Rutile type structural of $TiO_2$ also is a tetragonal crystal structure and this type used as white pigment in paint. Brookite type structural of TiO2 is an orthorhombic crystalline structure. Therefore, $TiO_2$ is had applications in various products such as solar cells, capacitors, paint pigments, sunscreen lotions and electrochemical electrodes [5]. $TiO_2$ is usually better in the anatase phase because of its high photocatalytic activity. Also, $TiO_2$ at anatase phase was found to be a superior photocatalytic material for purification and disinfection of water and air, as well as remediation of hazardous waste [6].

This material has been drawing quickly increasing attention from researchers because of its potential in magneto-electronic applications

* Corresponding Author Email: v.rafee@gmail.com

[7-9]. TiO2 doped with Fe, [10] Co, [11] Mn, [12] and other elements have been prepared by hydrothermal [13], synthesis spray under heat [14], sol-gel of spin coating [15], dip-coating [16], magnetron sputtering RF [17] and other methods. [18-20]

Recently, dilute magnetic semiconductor (DMS) is the main subject in the magnetic semiconductor field. This is made based on semiconductors that were doped with transitional metals. They are semiconductor substances that present good magnetic and semiconductor properties and they have been used widely for spintronic device [21]. Also, $TiO_2$ -based diluted magnetic semiconductor (DMS) with room temperature ferromagnetism was successfully prepared by Matsumoto et al. [22]

In this paper, we investigated the effect of doping percent on structural, optical and magnetic properties of the nanoparticles by preparing $TiO_2$ nanoparticles prepared by the sol-gel method at anatase phase and then these doped with the various percent of Mn.

## EXPERIMENTAL

*Preparation of Sol-gel $TiO_2$ and Mn-doped $TiO_2$ nano powders*

Sol-gel method and thermal treatment at 500$^0$C were used to make Mn-doped $TiO_2$ nano powder for 2hrs. Titanium isopropoxide (Merck, 99% Ti [OCH $(CH3)_2]_4$) was used as a precursor. The process was as follow. First, we added 4.23 ml titanium isopropoxide to 20 ml ethanol and kept it for 30 min at room temperature under magnetic stirring (magnetic magnet and stirrer Hot Plate Model Genway 1000) to obtain initial precursor solution. Then we combined.0.26 ml distilled water, 3.4ml Acetic acid (Merck, 99.9%) and 5 ml ethanol and added it to the initial solution with the rate one drop per second while it was under constant magnetic stirring. After that we added a predetermined quantity of Mn $(NO_3)_2$ to $TiO_2$ sol and stir it for one hour to obtain Mn-doped $TiO_2$ anatase nano powder. The quantity of the additive matter is estimated as follows [23]:

$$\%N_{Mn} = \frac{N_{Mn}}{(N_D + N_{Ti})} \quad (1)$$

Where, $N_{Ti}$ and $N_{Mn}$ are mole values of Ti and Mn respectively.

In the following, the prepared samples were transmitted to the furnace (electric furnace with the maximum operating temperature 1100°C model Thermal Defign, Lenton) and kept under thermal treatment at 500°C for 2hrs because in this temperature the dominant phase is Anatase [24].

Regarding that anatase phase of $TiO_2$ is the desired phase and it is dominated at 500°C and when the temperature of annealing is increased the anatase phase changes to rutile phase [25], therefore maximum temperature remains constant at 500°C.

## RESULTS AND DISCUSSION

*The structure of Mn-doped TiO2 nano powders*

X-ray power diffraction analysis (XRD) was done to study crystallite and phase structure of Mn-doped $TiO_2$ anatase, powder samples $Ti_{1-X}Mn_xO_2$ in which Mn is transition metal and x is the concentration of the additive matter (x=0%, 0.2%, 1%, 5%). This analysis was done using XRD analysis (model X pert, made by Philips Company doping and model Seifert 3003). Since the anatase phase was dominated at 500°C, the diffraction pattern of all samples confirm the presence of $TiO_2$ anatase phase as a dominate phase in the system which was in good agreement with Standard Card 1272-021-00 related to $TiO_2$ anatase phase and there is no additive peak related to another phase next to this phase [26]. This agreement is well seen in Fig. 1-a.

As it known from XRD results, XRD peaks have become broader by increasing concentration additive from 0.2% to 5%. In the most of the cases, broadening is due to decrease the grain size and structure disordering [27-28]. The size of the crystallites estimated by using Debye-Scherer's relationship [29].

$$D = \frac{k\lambda}{\beta \cos\theta} \quad (2)$$

The Fig. 1-a shows that the position of the peaks in the pure and Mn doped of the XRD pattern slightly shifted by changes in Mn percent of the sol. Also, the results are given in Tab.1.

Also, crystal lattice constants for planes 004 and 101 are measured as fallows [30].

$$\frac{1}{d^2} = \frac{h^2}{a^2} + \frac{k^2}{b^2} + \frac{l^2}{c^2} \quad (3)$$

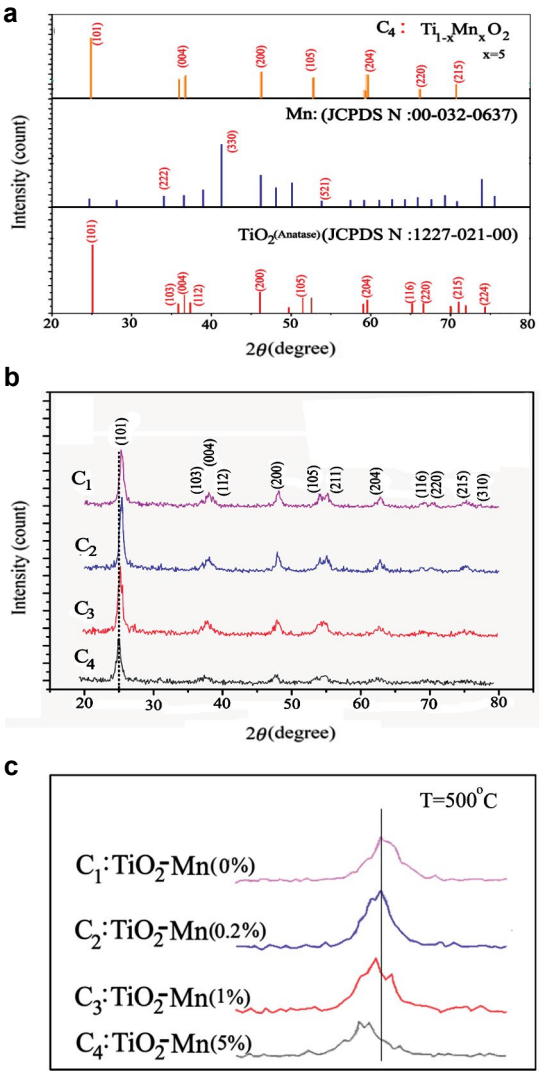


Fig. 1. X-ray diffraction spectrum,(a) Standard Card of $TiO_2$ anatas phase, Mn and peaks of $C_4$ sample (b)$Ti_{1-x}Mn_xO_2$ nano powder annealed at 500 °C related to the samples with different percent Mn, sample $C_1$: x=0%, sample $C_2$: x=0.2%, sample $C_3$: x= 1%, sample $C_4$: x= 5%. (c) The shift of peaks via Mn percent.

Table1. the lattice constants and the average size of the sample crystallites

| Sample | Mn –doped (%) | Lattice constants (□) | | D(nm) |
|---|---|---|---|---|
| | | a=b | c | |
| $C_1$ | 0 | 3.7689 | 9.4992 | 13.38 |
| $C_2$ | 0.2 | 3.7623 | 9.4548 | 13.03 |
| $C_3$ | 1 | 3.7621 | 9.3251 | 12.16 |
| $C_4$ | 5 | 3.7620 | 9.2125 | 11.36 |

Where, d is distance between continuous crystal planes, (hkl) is Miller index which shows crystal growth direction and a,b,c are lattice constants that are as follow for anatase: a=b≠c

The average size of the crystallite was 13.38nm, 13.03nm, 12.16nm and 11.36nm for samples $C_1$, $C_2$, $C_3$ and $C_4$ respectively. By comparing the average size of the crystallites, we find that increasing the percent of Mn leads to decrease the size of the crystallites.

The ionic radius of the $Mn^{4+}$ (0.670) as an addative in the octahedral site is smaller than the ionic radius $Ti^{4+}$(0.745), so $Ti^{4+}$ can replace with the $Mn^{4+}$ cation in the $TiO_2$ lattice. As a result, the decrease of the lattice constant C in the Mn-doped sample lattice can be due to the smaller ionic radius of Mn [31].

The X-pert analysis of X-ray diffraction spectrum of sample $C_4$ shows at Fig. 2. The presence of manganese is well confirmed by Fig. 2.

Considering XRD spectrums, it is clear observable that when the percent of Mn increase, the anatase peaks move toward to decrease 2θ [32].

*Morphology of Mn-doped TiO2 nano powders*

SEM analysis was used to study morphological properties of the surface and also calculate the average size of the nano particles (scanning electron microscope SEM, Model S4160, made by Hitachi Company). Fig. 3 shows SEM results.

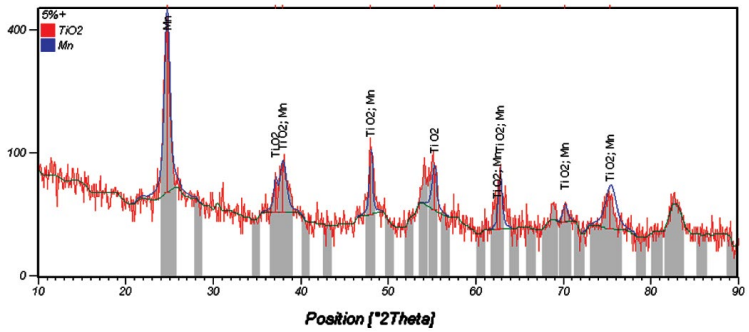


Fig. 2. X-ray diffraction spectrum of $Ti_{1-x}Mn_xO_2$ nano powder annealed at 500 °C related to the samples with Mn, sample $C_4$: x= 5%.

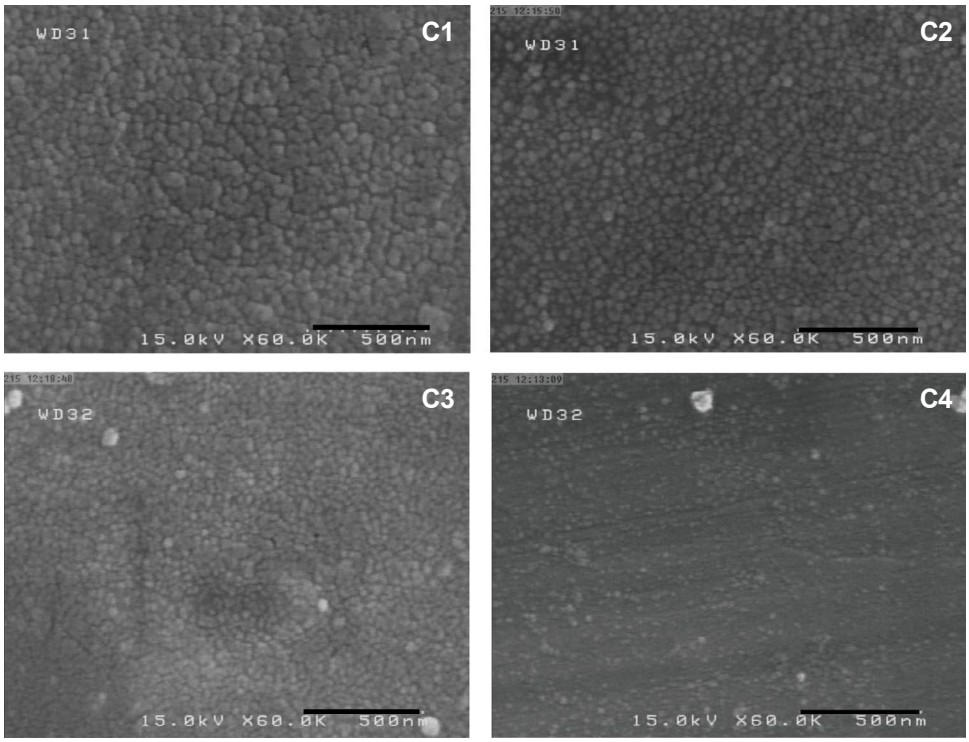


Fig. 3. SEM images of the annealed $Ti_{1-x}Mn_xO_2$ at 500 °C and with different concentrations of the Mn: C1=0%, C2=0.2%, C3= 1% and C4=5%.

As can be seen, the grain size is influenced by changing of a percent of Mn. The average size of the grain is 20, 25, 28 and 30nm for C1, C2, C3 and C4 respectively. These results show that the decrease grain size is due to the increase of the percent of Mn which is in agreement with the results of the obtained crystallites size by the XRD.

Fig. 4 show the approximated average size of the particles using SEM device based on the percent of Mn respectively.

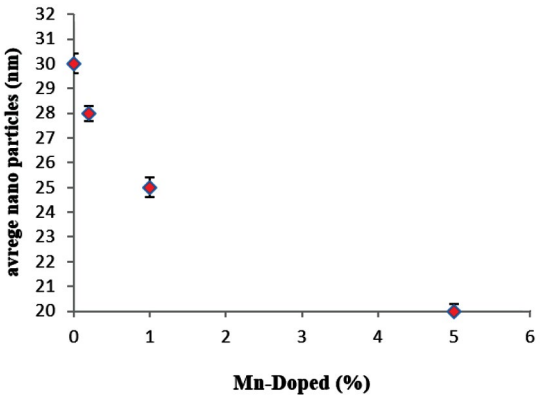


Fig. 4. the average size of the nanoparticles with different Mn content.

*Optical properties of Mn-doped TiO2 nano powders*

UV-Vis spectrophotometer (Model Varian-Cary 500Scan) was used to calculate the optical energy band gap of the samples.

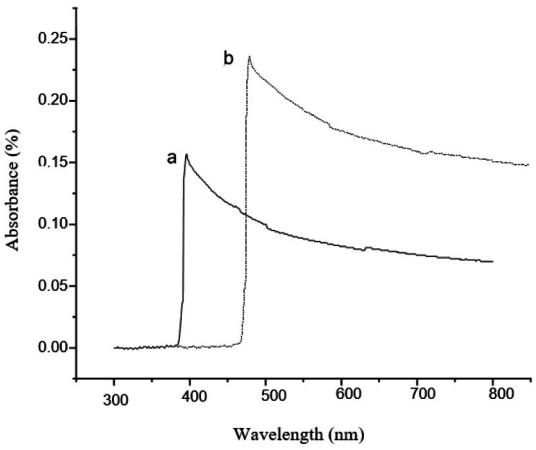


Fig. 5. the UV-Vis absorption spectra of (a) $TiO_2$ pure nano powder (b) $Ti_{1-x}Mn_xO2$ nano powder with the percent of Mn equal to 5% annealed at 500 C.

Fig. 5 shows the absorption of the $TiO_2$ pure

and $Ti_{1-x}Mn_xO_2$ nano powders (Mn-doped $TiO_2$ nano powder) with the percent of Mn equal to 5%. These samples annealed at 500°C. As you see $TiO_2$ pure nano powder shows the absorption maximum at 380-390nm of the absorption area while $TiO_2$ nano powder synthesized with Mn with the 5% concentration has an absorption maximum at the 480-490nm.

The optical energy band gap of the samples calculated as fallowing relation [33]:

$$E = h\nu = hc/\lambda \quad (4)$$

Where, $h$ is the plank constant ($h$=6.62 ×10 $^{-34}$), $c$ is the light speed (c= 3× $10^8$ m/s) and $\lambda$ is the wavelength maximum. The amount of estimated energy gap for the $TiO_2$ pure nano powder based on λ=388nm is E=2.3Ev while it is E=6.2 eV for the synthesized $TiO_2$ nano powder with 5% concentration of the Mn based on λ= 480nm. This show that by doping Mn ions at samples and by considering the different ionic radius of the Mn and $TiO_2$, the variation between valance band and the conduction band of $TiO_2$ lead to change the band gap and shift the absorption edge toward the visible area [34]. A number of band gap decreases [35-37] and this change lead to increase the photocatalytic sensitivity of the $TiO_2$ [36].

*Magnetic properties of Mn-doped TiO2 nano powders*

After investigating the magnetic behavior of the samples using VSM, we reported that $Ti_{1-x}Mn_xO_2$ nano powder samples with the Mn concentrations 1%, 0.2% and 0%, annealed at 500°C do not show reasonable magnetic behavior, while the sample show paramagnetic behavior by increasing the Mn concentration to 5%. Fig. 6 describes the magnetic hysteresis (M-H) for $Ti_{1-x}Mn_xO_2$ nano powder with the Mn concentration at %5 and annealed at 500°C. This sample has effective field $H_C$ 20.43Oe and its hysteresis is 1.61×$10^{-5}$ *emu*/g. Since The $TiO_2$ do not show the magnetic properties, so the observed paramagnetic can be due to the bond of the Mn ions to $TiO_2$ lattice. According to the obtained results from XRD spectrum of the samples in this research that show the $Ti^{+4}$ replaced with $Mn^{+4}$ at $TiO_2$ lattice, it can be concluded that Mn ions substitution in $TiO_2$ lattice can be the reason for the paramagnetic behavior. Also not observing magnetic behavior with the concentration less than 5% can be due to the little Mn concentration because it cannot create the magnetic order for the samples.

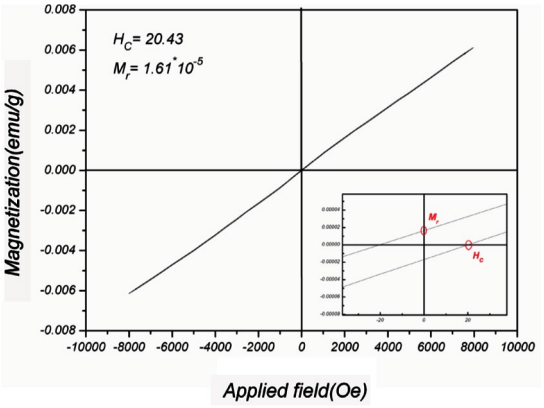


Fig. 6. The chart of the magnetization variations as a function of M-H forcing of the $Ti_{1-x}Mn_xO_2$ nano powder with x=5% at the room temperature.

*The composition of Mn-doped TiO2 nano powders*

EDX was used to study chemical composition and chemical analysis energy. The Mn concentration was measured using EDX analysis. Fig. 7 shows the typical spectrum of the EDX analysis for the powder sample with 5% concentration. This confirms the presence of Mn in the structure which indicates $Ti^{+4}$ replaced by $Mn^{+4}$ in the $TiO_2$ lattice.

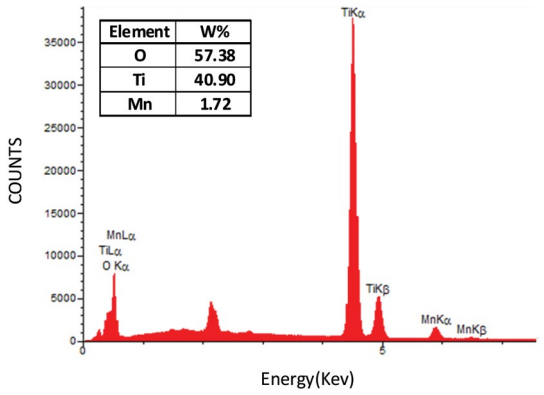


Fig. 7. EDX image of $Ti_{1-x}Mn_xO_2$ nano powder with 5% of the Mn concentration and annealed at 500 C.

## CONCLUSIONS

In this paper, structural, magnetic and optical properties of $TiO_2$ nanoparticles are studied by

preparing them with doping percent 0, 0.2, 1 and 5% using the sol-gel method. The results of the X-ray diffraction analysis confirm the anatase phase of the samples and show that when the doping percent increases, the size of nanoparticles significantly decreases because the ionic radius of the Mn is smaller than that of the Ti. Also SEM results show that as the doping percent increases, the surfaces are smoother and they will have a thinner gradation. The increase in the average size of the particles confirms the X-ray diffraction results. In the following, EDX results confirm Mn-doping at the samples. The analysis of the absorption spectrum of the spectrophotometry for the samples with %5 Mn-doping and samples without doping show the displacement at the absorption maximum of the pure nano powder from 380-390nm than to the doped samples with 5% Mn concentration at 480-490nm. Also, results related to the energy gap estimation show the decrease band gap from 2.3 eV to 2.6 eV for the pure sample and the doped sample with 5% Mn, respectively. At last, as the VSM show that the samples without doping and the samples with doping do not indicate significant paramagnetic properties at 0, 0.2 and 1%. But the doping with 5% of the sample not only shows good paramagnetic properties but also it has effective field $H_C$ 20.43Oe and magnetic hysteresis is $1.61\times10^{-5}$ *emu*/g emu.

## CONFLICT OF INTEREST

The authors declare that there is no conflict of interests regarding the publication of this manuscript.

## REFERENCES


1. J. P. Hsu, and A. Nacu, Langmuir 19(10), 4448-4454 (2003).
2. H. Irie, Y. Watanabe, and K. Kazuhito Hashimoto, Chemistry Letters 32(8), 772-773 (2003).
3. D. Nezameddin, D. Salari, and M. A. Behnasuady, Iran. J. Chem. Chem. Eng. (IJCCE), 21(1): 55-65 (2002).
4. G.L. Puma, A. Bono, D. Krishnaiah, and J.G. Collin, J. Hazard. Mater., 157(2-3), 209-219 (2008).
5. G. Meacock, K.D. Taylor, M.J. Knowles, and A. Himonides, J. Sci. Food Agric., 73(2), 221-225 (1997).
6. H. F. Yu, Z. W. Zhang, and F. C. Hu, J. Alloy. Compd, 465(1-2), 484-490 (2008).
7. J. E. Nam, H. J. Jo, D. H. Son, D. H. Kim, and J. K. Kang, Appl. Mech. Mater, 705, 320-323 (2015).
8. W. Weng, T. Higuchi, M. Suzuki, T. Fukuoka, T. Shimomura, M. Ono, L. Radhakrishnan, H. Wang, N. Suzuki, H. Oveisi, and Y. Yamauchi, Angewandte Chemie,122(23), 4048-4051(2010).
9. W. Chen, X. Tao, J. Zhang, Q. Fang, and J. Yang, J. Am. Ceram. Soc, 88(11), 2998-3002 (2005).
10. AA Firooz, BH. Nia, J. Beheshtian, M. Ghalkhani, J. Elect. Math, 46 (10) 5657-63 (2017).
11. A. Eslami, M. M. Amini, A. R. Yazdanbakhsh, A. Mohseni-Bandpei, A. A. Safari, and A. Asadi, J. Chem. Tech. Biotechn, 91(10), 2693-2704 (2016).
12. X. Ning, X. Wang, X. Yu, J. Zhao, M. Wang, H. Li, and Y. Yang, Sci. Rep, 6, 22634 (2016).
13. Z. Yang, B. Wang, H. Cui, H. An, Y. Pan, and J. Zhai, J. Phys. Chem. C, 119(29), pp.16905-16912 (2016).
14. S. Dhanapandian, A. Arunachalam, and C. Manoharan, J. Sol-Gel. Sci. Techn, 77(1), 119-135 (2016).
15. H. Affendi, I. Hidayanti, A. Azhar, N. Ezira, M Saad., P. Sarah, and M. Rusop, Adv. Mat. Res, 1109 529-533 (2015).
16. F. H. Ali, W. A. Twej, and A. Al-Khafaji, J. Spectrosc. Mol. Phys, 10(10), 91-96 (2015).
17. K. Safeen, V. Micheli, R. Bartali, G. Gottardi, and N. Laidani, J. Phys. D. Appl. Phys, 48 (29), 295201 (2015).
18. P. Mazzolini, V. Russo, C. S. Casari, T. Hitosugi, S. Nakao, T. Hasegawa, and A. Li Bassi, J. Phys. Chem. C, 120(33), 18878-18886 (2016).
19. A. R. Bahramian, Iran. J. Chem. Chem. Eng. (IJCCE), 35(2), 27-41 (2016).
20. A. R. Allafchian, S. A. H. Jalali, R. Amiri, and S. Shahabadi, J. Mater. Sci: Mater-El, 28(16), 12312-12319 (2017).
21. T. Dietl, and H. Ohno, Rev. Mod. Phys, 86(1), 187 (2014).
22. Y. Matsumoto, M. Murakami, T. Shono, T. Hasegawa, T. Fukumura, M. Kawasaki, P. Ahmet, T. Chikyow, S. Y. Koshihara, and H. Koinuma, H., Science, 291(5505), 854-856 (2001).
23. P. I. Gauma and M. J. Mills, J. Am. Ceram. Soc., 84, 619-622 (2001).
24. O. Ergün, O. Karslioğlu, A. Yilmaz and D. Üner,, Turk. J. Chem., 31, 501-508 (2007).
25. A. Razeghizadeh, E. Elahi, and V. Rafee, Nashrieh Shimi va Mohandesi Shimi Iran, 35(2), 1-8 (2016).
26. H. Lin, C. P. Huang, W. Li, C. Ni, S. I. Shah and Y. H. Tseng, Appl. Catal. B, 68, 1 (2006).
27. P. Sahu, M. De and M. Zdujić, J. Mater. Chem. Phys, 82, 864-876 (2003).
28. V. Sepelák, U. Steinike, D. Chr. Uecker, S. Wibmann and K. D. Becker, J. Sol. St. Chem., 135, 52-58 (1998).
29. A. Razeghizadeh, M. Mahmoudi Ghalvandi, F. Sohillian, and V. Rafee, Phy. Chem. Res, 5(3), 497-504 (2017).
30. J. K. Saha, and J. Podder, J. Bangl Acad. Sci, 35(2), 203-210 (2011).
31. D. Peng, L. Fa-Min, Y. Xin-An, and L. Jian-Qi, Chinese Physics B, 17(2), 72 (2008).
32. C. R. Estrellan, C. Salim and H. Hinode, React. Kinet. Catal. Lett. 98, 187-192 (2009).

33. A. Razeghizadeh, L. Zalaghi, I. Kazeminezhad, V. Rafee. Iran. J. Chem. Chem. Eng. (IJCCE), 36(5) 1-8 (2017).
34. Y.L Dong, J. L Won, S. Jae Sung et al, Comput. Mater. Sci, 30, 383-388 (2004).
35. D. L. Gomathi, K. Nagaraju, M. B. Narasimha, K. S. Girish, J. Molec. Catal. A: Chem 328, 44-52 (2010).
36. T. Umebayashi, T. Yamaki, H. Itoh, K. Asai, J. Phys. Chem. Solids, 63, 1909-1920 (2002).
37. W. Choi, A. Termin, M. R. Hoffmann. J. Phys. Chem. 98, 13669-13679 (1994).